PAPER AAS 94-134

A First Look at Orbit Determination for the Cassini Mission

Part 2: Saturn Tour

Anthony H. Taylor, Rodica Ionasescu, and Robin M. Vaughan

Jet Propulsion Laboratory
California Institute of Technology
Pasadena, CA

AAS/AIAA Space flight Mechanics Meeting

COCOA BEACH, FLORIDA FEBRUARY 14-16,1994

AAS Publications Office, P.O. Box 28130, San Diego, CA 92198

AAS 94-134

A FIRST LOOK AT ORBIT DETERMINATION FOR THE CASSINI MISSION

Part 2: Saturn Tour

Anthony H. Taylor*, Rodica Ionasescu*, and Robin M. Vaughan*

This paper completes the presentation of the first round of orbit determination analysis accomplished as part of Cassini navigation studies. The thrust of the analysis was to characterize operational orbit determination accuracy to first order for selected phases of the mission. The previous paper, Part 1, covered early phases from inner solar system cruise through the approach to Saturn and delivery of the Huygens probe to Titan. Part 2 resumes chronologically where Part 1 left off, covering the tour phase after delivery of the Huygens probe. The paper first presents the rationale used to select tour orbits for the study. Then the analysis setup is described, including choice of data types and schedules and details of the filter configuration such as a priori uncertainties and data weights. Next, the baseline results consisting of trajectory and target knowledge uncertainties relative to Titan and Saturn at delivery times associated with each body are compared to the applicable project navigation requirements. Variations from the baseline, which include data failure scenarios, optimistic scenarios, and the use of enhanced radiometric data types, are also presented. The paper concludes with a discussion of the numerical difficulties experienced in attempting to map covariance matrices through multiple Titan encounters.

INTRODUCTION

This paper continues the presentation of results of the initial round of Orbit Determination (OD) analysis for the Cassini mission. The Cassini spacecraft is scheduled for launch in October of 1997 on a seven-year journey to Saturn. During the first orbit about Saturn in late 2004, the Huygens probe is released into Titan's atmosphere, Then the orbiter continues on a four-year tour of the Saturn system, A previous paper, Part 11, presented OD analysis results for early phases from inner solar system cruise through the approach to Saturn and delivery of the Huygens probe to Titan. This paper, Part 2, resumes chronologically where Part 1 left off, covering the tour phase after delivery of the Huygens probe. Emphasis is placed on first-order characterization of the operational orbit determination accuracy; the results are a representative snapshot of a continually evolving state of knowledge of Cassini orbit determination.

The Cassini Saturn tour includes numerous orbits designed to accomplish diverse scientific objectives with respect to Saturn and it's rings, Titan, and the other icy satellites. Figure 1 shows the 63 orbits of a representative tour design. These orbits cover a wide range of periods, orientations with respect to the Sun and Earth and inclinations with respect to the Saturn equatorial plane. The orbital variations in the tour trajectory are primarily shaped by the spacecraft's interactions with Titan's substantial gravitational field. Each Titan encounter is designed to perturb the trajectory in a desirable way for the next orbit and to return the spacecraft to Titan after onc or more revolutions about Saturn. Trajectory Correction Maneuvers

(TCMS) are executed throughout the orbits to maintain the desired encounter geometry. The last opportunity to "fine tune" this geometry occurs at the TCM scheduled a few days prior to each Titan flyby. Any small pre-encounter trajectory errors remaining after this TCM are amplified by Titan's gravitational field into large post-encounter errors in targeting to the next Titan flyby. A clean-up TCM is inserted after each encounter to correct these residual errors, Larger errors for the pre-encounter maneuvers will greatly increase the size of the clean-up maneuvers, causing premature depletion of maneuvering fuel and early end of the mission. Minimizing pre-encounter navigation errors is thus one of the major challenges for operational Orbit Determination (OD). Other challenges arise from the need to provide trajectory predictions for the design of the science encounter sequences, the necessity for rapid determination of the post-encounter trajectory in order to design the clean-up TCM, and requirements from science to provide accurate reconstructions of each encounter.

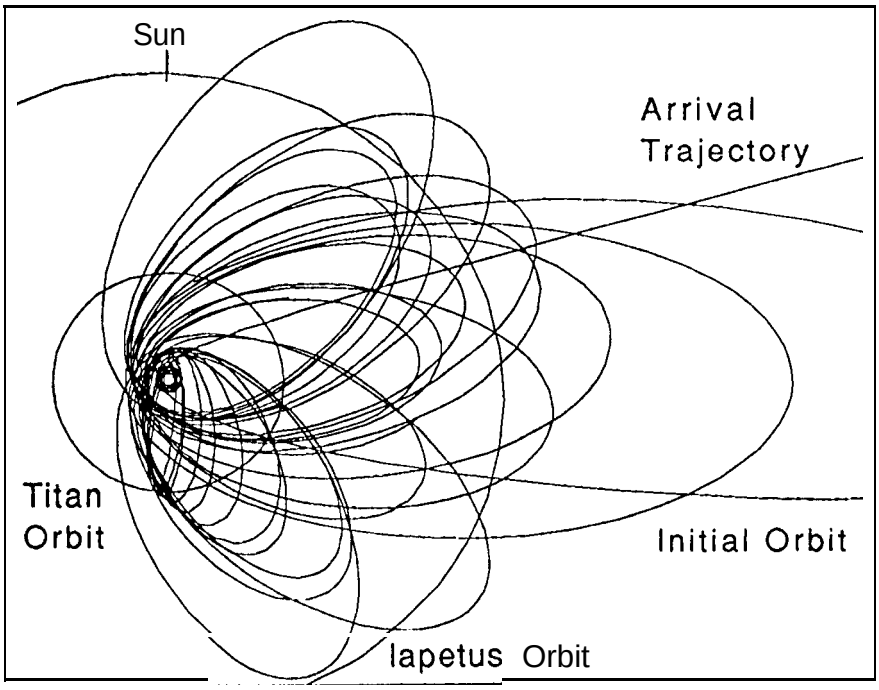

Figure 1 Spacecraft Orbits for a Typical Saturn Tour, (Orbits are shown in a rotating coordinate system in which the Sun direction is fixed.)

The methodology for the tour OD analysis discussed here is similar to that described in Reference 1 for the analysis of the other mission phases. Representative orbits were selected to characterize OD capabilities over the entire tour. Covariance analyses were performed to generate OD uncertainties for these orbits using simulated data in an epoch state, linearized least squares formulation employing a batch sequential filter (similar to operational OD software). The details of the analysis setup arc given in the next section. The rationale and nomenclature used in selecting orbits for study are discussed along with the choice of data types and schedules and the filter configuration including a priori uncertainties and data weights. Following that, baseline results are presented for the OD deliveries associated with each Titan encounter. Saturn-relative results, associated with orbit periapses, are also discussed. Then, variations on the baseline are described, including both pessimistic scenarios such as the complete loss of optical data and optimistic scenarios such as the availability of enhanced radiometric data types. Numerical errors that occurred for some cases when mapping covariance matrices through multiple Titan encounters are also discussed. Conclusions and recommendations for future work are presented in the final section.

ANALYSIS SETUP

Orbit Selection

It was neither possible nor desirable to study every orbit in the entire tour. The resources were not available, but more importantly, the tour will be changed from the design shown in Figure 1 before Cassini arrives at Saturn, Since specific results for all orbits in the present tour design would inevitably become obsolete, it was decided to select only a few representative trajectory arcs. Each arc would span two consecutive Titan encounters; the arc would begin shortly before one encounter and end just after the following encounter. The selection of these arcs would be based on certain parameters to which the OD process was expected to be sensitive. These parameters include the phase angle* of the satellite images as seen by the spacecraft, the placement of the Titan encounters relative to the periapsis of the spacecraft orbit, the orbital inclination relative to Saturn's equator, and the ratio of spacecraft orbits to Titan orbits between Titan encounters. Phase angle is of concern because large errors are expected in processing optical navigation frames with high-phase Titan images. The accuracy of current models of the reflectance properties of Titan's atmosphere degrades significantly as the phase angle approaches 180 degrees. It was hypothesized that the location of the Titan encounter relative to Saturn periapsis would cause differences in OD performance depending on whether or not the solutions were mapped through Saturn periapsis prior to the encounter. The effects of the other parameters on the OD accuracy were unknown but considered potentially significant,

The initial orbits for the tour are positioned such that the planet and satellites are viewed at relatively low phase angles by the spacecraft. Over the four years of the tour, the line of apsides of the spacecraft orbit rotates such that near the end of the tour the satellites arc viewed at very high phase angles. The tour is broadly divided into "Low-phase" and "High-phase" portions, with the division arbitrarily placed at the point where the angle of the line of apsides with the sun line reaches 135 degrees. A similar situation occurs for orbital inclination with the initial orbits having small inclinations and orbits toward the end of the tour having inclinations approaching 90 degrees. The transition from "Low" (near zero) to "High" inclination takes place at about the same time as the transition to high phase. The trajectory arcs selected for the OD analysis thus clustered into two groups, those occurring in the early portion of the tour and those occurring in the latter portion.

The current tour design is also characterized by multiple occurrences of Titan encounters placed before and after Saturn periapsis. Encounters occurring while Cassini is inbound to Saturn periapsis are called, appropriately, "Inbound" encounters. These generally occur about two days before Saturn periapsis. Similarly, "Outbound" encounters occur about two days after periapsis. Examples of each possible pairing of inbound and outbound encounters can be found for any two consecutive Titan encounters in the tour. There is also considerable variation in the ratio of the number of Titan orbits to spacecraft orbits between Titan encounters. The term "resonance" is used since this ratio can always be expressed as the quotient of two integers. A previous tour design contained 12 different resonances, the most plentiful of which were 1:1 (7), 2:1 (8), 3:1 (5) and 3:2 (5). Although the selected arcs did not cover all possible combinations of inbound and outbound encounters or values for the resonance ratio, they did provide a reasonable sample of these parameters.

The final set of five arcs chosen for this OD analysis arc described in Table 1. The following nomenclature is introduced to distinguish among the different arcs: the arc names consist of 5 characters, ABCnm, where A = L(ow) or H(igh) phase/inclination, B = I(nbound) or O(utbound) for the first Titan encounter, C = I(nbound) or O(utbound) for the second Titan encounter, n = number of Titan revolutions between encounters, and m = number of spacecraft revolutions between encounters.

As previously mentioned, the spacecraft trajectory used in the OD simulation begins near onc Titan flyby and continues to a few days beyond the next Titan flyby. The first encounter is included to aid in the initialization of the OD solution, while the second encounter is the onc for which OD results will be

* The phase angle is the spacecraft - target body - sun angle.

presented.* Depending on the resonance ratio, one or more Saturn apoapses and periapses occur between these flybys. The navigation events considered as part of the simulation include three types of statistical maneuvers and several OD data cutoff times. The maneuvers are scheduled at the Saturn apoapsis prior to a Titan flyby, 3 days prior to the flyby, and 2 days after the flyby. The apoapsis maneuver corrects errors remaining since the previous Titan encounter. The Titan delivery maneuver at T-3 days uses improved OD knowledge since apoapsis to trim for the flyby, and the Titan clean-up maneuver at T+2 days reduces trajectory dispersions in preparation for the next flyby. OD data cutoff times were placed at 1 day before each maneuver (2 days for the apoapsis maneuver) for purposes of maneuver design, 2 days before the Titan flyby for science knowledge updates and 4 days after the flyby for reconstruction, Examples of the timeline and spacecraft trajectory for arc LO021 are given in Table 2 and Figure 2.

Table 1. GEOMETRY PARAMETERS FOR SELECTED TRAJECTORY ARCS

Trajectory	Description	Sun Phase Angle (degrees)	Orbit inclination (degrees)	Titan Periapsis Altitude (km)
LOO21	Low phase, low inclination, outbound to outbound orbit, 2:1 Titan-S/C resonance	56	7	950
LII21	Low phase, low inclination, inbound to inbound orbit, 2:1 Titan-S/C resonance	52	7	1200
LIO31	Low phase, low inclination, inbound to outbound orbit," 3:1 Titan-S/C resonance	53	0	4000
HII32	High phase, high inclination, inbound to inbound orbit, 3:2 Titan-S/C resonance	167	15	950
HII11	High phase, high inclination, inbound to inbound orbit, 1:1 Titan-S/C resonance	172	47	950

Table 2. TIMELINE FOR EVENTS IN TRAJECTORY ARC LO021

Event Time (Days from 2nd Titan Flyby)	Event
-36	Trajectory start
-34	Saturn periapsis
-32	1st Titan flyby
-20	Data cutoff for maneuver
-18	Saturn apoapsis and maneuver
-4	Data cutoff for maneuver
-3	Titan Delivery Maneuver
-2	Data cutoff for encounter design (science knowledge update)
-2	Saturn periapsis
0	2nd Titan flyby
+1	Data cutoff for maneuver
+2	Titan Clean-Up Maneuver
+4	Data cutoff for reconstruction

* This reflects current thinking on how to conduct OD operations; after each Titan encounter the arc is advanced by dropping the previous encounter and extending the nominal trajectory past the next encounter.

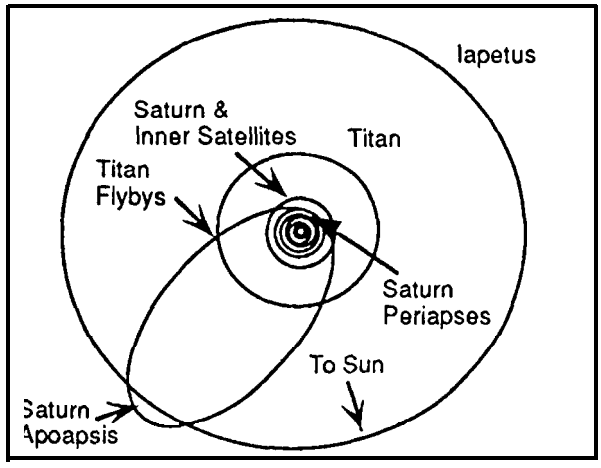

Figure 2 Orbit Geometry for Trajectory Arc LOO21

Data Types and Schedules

A mix of radiometric and optical data types was used for the tour OD simulations. The data schedule for a typical baseline case is summarized in Table 3. Standard Doppler and ranging were the only radiometric data included in the baseline cases. More sophisticated radiometric data types — including high-precision ranging, difference Doppler, and ADOR — were used in variations on the baseline cases and are discussed in a later section. A gap was placed in the radiometric data arc around the time of Titan closest approach to allow for science observations. The optical data included pictures of Titan and five of the other icy satellites against the star background taken with the spacecraft's narrow-angle camera (NAC). Only six of the nine major satellites could be used as optical targets in the OD simulation due to a limitation in the software. * Titan optical data was omitted for the 4-5 days around each Titan flyby to avoid the large perturbations due to the increase in centerfinding errors as the size of the satellite increases in the camera field-of-view. Even if centerfinding error size were not a concern, it would be difficult to obtain Titan optical navigation pictures for at least part of this time since a star could not bc captured in the same field-of-view with the large satellite image.

Table 3. OPTICAL & RADIOMETRIC DATA SCHEDULES

Data Types	Schedule	Comments
	Optical	
General	3-4 pictures/day	Use narrow-angle camera (NAC)
Titan	Average 1/3 of total number of images No Titan pictures from T-3 days to T+2 days for inbound orbits T-2 days to T+3 days for outbound orbits	Limit OD errors due to centerfinding errors
Icy Satellites	Average 2/3 of total number of images	Enceladus, Tethys, Dione, Rhea, Iapetus; approximately same number of images for each satellite
	Radiometric	
Doppler & Ranging	1 pass/day 1 measurement/hour Continuous coverage from T-1 day to T-I2 hours & T+8 hours to T+16 hours	Coverage as needed from each of the three Deep Space Network tracking sites

* This limitation will be removed in the operational version of the OD software.

Filter Configuration

The filter configuration for the tour OD simulations is summarized in Tables 4 and 5. Table 4 lists the filter parameters along with the assumptions for the a priori covariance. The parameters are separated into estimated and "considered" categories where the "considered" parameters simulate systematic errors in modeling which are not improved by the filter. Table 5 gives the weights for the different data types used in the baseline cases. It should bc noted that the filter setup evolved in parallel with the simulations for the different trajectory arcs. The assumptions given in the tables were used for arc HII32. A priori covariances and data weights for some of the other arcs differed from these assumptions in certain areas. These differences will be noted where significant in the sections that follow.

The primary source of the non-gravitational accelerations included in the spacecraft model used by the filter is attitude control activity. Cassini is a three-axis stabilized spacecraft, using either attitude control thrusters or momentum wheels to maintain attitude. The thrusters are unbalanced so that when they are in use there is a small average daily acceleration on the spacecraft. When the momentum wheels control the attitude, the thrusters arc used periodically to desaturate the wheels. The desaturation events generate small AVS which can also be approximated by an average acceleration. Non-gravitational accelerations due to momentum wheel desaturation activity and thruster firings for spacecraft attitude control were divided into two components: a process-noise component which is estimated stochastically and a "considered" bias component,

A simple conic model was used for the satellite orbits where a satellite's position and velocity is determined from its position and velocity at an epoch time, its mass and the Saturn system mass. These parameters were all estimated and their a priori covariance was specified as a single partition of the overall filter a priori covariance matrix. In order to simulate the retention of ephemeris knowledge from previous tour orbits combined with many years of earth-based astrometric data, satellite a priori covariances were generated in a two-step process. First, a solution was run on one of the data arcs using large a priori epoch state uncertainties. Next a mean motion constraint representing earth-based ephemeris knowledge was applied to the covariance computed by the filter. This resulted in an a priori covariance with correlations between all satellite parameters except between satellite masses,

The filter also included parameters related to the data, For the optical data, a constant centerfinding error proportional to the diameter of the satellite image was considered. This was used to represent the mismodeling that can occur in the process of extracting satellite centers from the optical frames, The modeling is difficult and complex for a body with an atmosphere such as Than, and for this reason the Titan centerfinding errors are larger than for the icy satellites, Also, for Titan, the accuracy of the centcrfinding algorithms degrades at high phase angles, The a priori uncertainties for Titan ccnterfinding errors are thus larger for the high-phase trajectory arcs.

The assumptions on data quality are specified in Table 5 as 1σ measurement noise values. The corresponding "data weight" used by the filter is the reciprocal of the square of this uncertainty. The values chosen for standard Doppler and ranging data are conservative since this is the first assessment of tour OD capabilities. A similarly conservative, constant value was initially chosen for both Titan and the icy satellite optical data, A new strategy was later adopted for the Titan optical data weight due to large growth in the Titan-relative uncertainties induced by the centerfinding error consider parameters in the last few days before the Titan encounter. The trajectory error corresponding to a constant Titan data weight decreases as the spacecraft range to Titan decreases, while the trajectory error associated with the centerfinding consider parameters remains a fixed percentage of Titan's diameter. For pictures taken near the flyby, the error implied by the constant data weight became much smaller than the error due to the consider parameters, inflating the OD uncertainties. The new weighting scheme for Titan optical data varied the data weight as a function of range to Titan in order to match the assumed size of the measurement error in pixels to the size of the considered centerfinding error in pixels. Such a deweighting procedure would be used by OD analysts in actual operations if the currently available centerfinding techniques were used for the Titan images.

TABLE 4: A PRIORI UNCERTAINTIES FOR THE SATURN TOUR **OD** ANALYSIS

Parameters	10 A Priori Uncertainty
Estimated Constant Parameters	
Spacecraft state	
position per axis	150 km
velocity per axis	60 mm/s
Saturn ephemeris	
RSS position sigma	1200 km
RSS velocity sigma	9.2 xl 0^{-6} km/s
System mass (GM)	100 km^3/s^2
Satellite masses (GMs)	
Enceladus	1.9 km^3/s^2
Tethys	3.4 km^3/s^2
Dione	7.1 km^3/s^2
Rhea	1.4 km^3/s^2
Titan	0.1 km^3/s^2
Iapetus	0.7 km^3/s^2
Saturn J2	0.001
Satellites (RSS position sigmas)	
Enceladus	397 km
Tethys	21 km
Dione	22 km
Rhea	15km
Titan	38 km
Iapetus	36 km
Maneuvers (nominal **AV)**	1.7°/0 of nominal ΔV
Apoapse (2 m/s)	34 mm/s
T-3 days (1 m/s)	17 mm/s
T+2 days (5 m/s)	85 mm/s
Estimated Stochastic Parameters	
Non-gravitational accelerations	2x1 0^{-12} km/s^2
Batch update	1 day
Correlation time	2 days
Considered parameters	
Non-gravitational accelerations	1 x 1 0^{-12} km/s^2
Solar pressure coefficients	Percentage of nominal acceleration
(3000 kg s/c, 15 m^2 nominal area, 0.34x 10-': km/s^2 nominal acceleration at Saturn)	11% radial 2%'$_0$ transverse
Optical Centerfinding Error	% of diameter
Titan	Low phase angle: 0.75% (40 km) High phase angle: 1.3% (65 km)
Icy satellites	0.29'0
Station location	
spin radius	50 cm
longitude	50 cm
z-height	580 cm
Transmission Media (X-band)	
Troposphere zenith delay	4.5 cm
Day-time ionosphere zenith delay	5 cm
Night-time ionosphere zenith delay	1 cm

TABLE 5. OPTICAL & RADIOMETRIC DATA SIGMAS

Data Type	Sigma
Optical	
Titan	0.5 pixel or matched to centerfinding error
Icy Satellites	0,5 pixel (1 pixel= 6 μrad)
Radiometric	
Doppler	0.5 mm/s
Ranging	0.5 km

BASELINE OD PERFORMANCE RESULTS

This section discusses the results for the baseline simulations for each of the five trajectory arcs. The presentation begins with a brief look at the overall behavior of the orbit uncertainty as a function of time for one of the sample trajectories. This is followed by more detailed discussions of the OD accuracies at the data cutoff times of T-4 days, T-2 days, and T+4 days. These cutoff times correspond to the last OD deliveries at which the project navigation requirements shown in Table 6 can be satisfied, The discussion for each OD delivery focuses on comparing the OD capabilities from the baseline simulations with the corresponding requirements.

TABLE 6. TOUR NAVIGATION REQUIREMENTS

Performance Measure	Requirement	OD Delivery
S/C Delivery to Titan Low-Phase Orbits High-Phase Orbits	Icr Titan B-plane error ellipse size ≤ 25 km 30 km	T-4 days (for final Titan targeting maneuver at T-3 days)
Nadir Pointing Prediction Titan & Saturn	95% confidence of pointing accuracy ≤ 1.9 mrad at altitudes >30,000 km ≤ 2.5 mrad at altitudes >20,000 km	T-2 days
Nadir Pointing Reconstruction Titan & Saturn	95% confidence of pointing accuracy ≤ 2.0 mrad at altitudes >10,000 km	T+4 days

OD Knowledge as a Function of Time

Figure 3 is an example of orbit uncertainty as a function of data cutoff time for the LII21 arc. Spacecraft state uncertainties are mapped to the Titan-centered B-plane at the time of closest approach for the second encounter. (See the appendix for an explanation of the B-plane.) The semi-major and semi-minor axes of a 1σ error ellipse in the B-plane are plotted along with the 1σ uncertainty in the time-of-flight. Locations of the apoapsis maneuver and the delivery maneuver at T–3 days are indicated. The figure shows that for most of the approach the error ellipse is long and thin, with an erratically decreasing size occasionally pumped up by the maneuver execution errors.

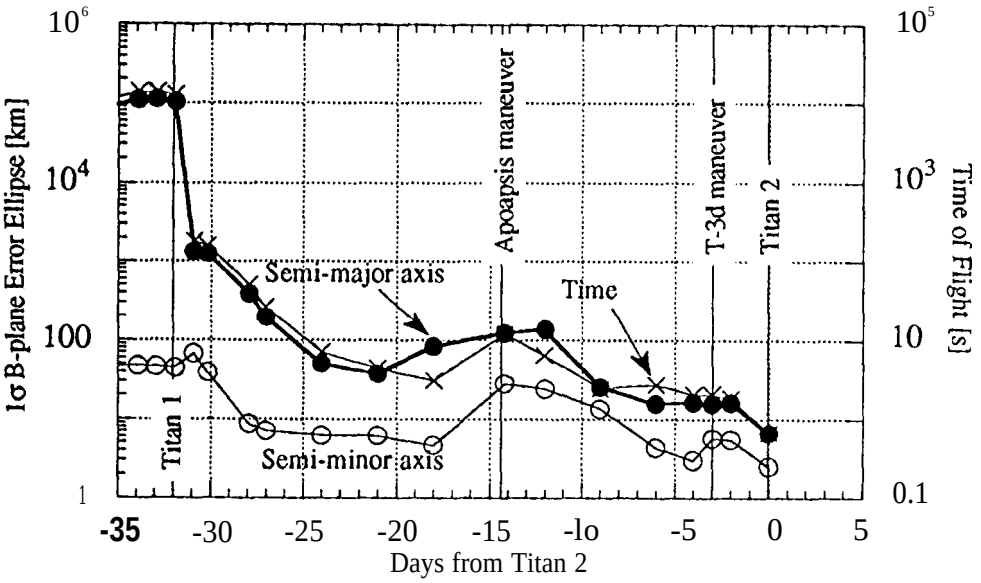

Figure 3 1σ B-plane Error Ellipse and Time-of-Flight Uncertainty as a Function of Data Cutoff Time from Titan Closest Approach for the LII21 Arc.

Titan - 4 day Knowledge for Titan Delivery Maneuver

One of the goals of this analysis was to determine delivery uncertainties in the Titan B-plane so that fuel costs for the post-Titan maneuvers could be obtained. Large delivery dispersions could cause premature depletion of maneuvering fuel and early end of mission. If OD uncertainties at the T-4 day delivery can be kept within the limit given by the first requirement shown in Table 6, there will be adequate fuel to complete the mission. Table 7 shows the B-plane error ellipse parameters and time-of-flight uncertainty at T–4 days for all five of the sample trajectories. Most of the arcs do meet the requirement on error ellipse size for the different types of orbits, but the values for the high-phase trajectories and for the LOO21 arc are very close to the size limit. The error ellipses themselves arc plotted on a composite Titan B-plane in Figure 4, The semi-major axes of the ellipses arc predominately in the plane of Titan's orbit and there is little variation in the size of this axis among the five arcs. However, the size of the semi-minor axis is larger for the high-phase, high-inclination trajectories, and the ellipse orientation for the HII32 arc is quite different. The reason for this behavior has not been investigated in detail.

TABLE 7. 1σ B-PLANE STATISTICS AT T-4 DAYS FOR THE 5 TOUR TRAJECTORIES

Trajectory	Semi-major Axis (km)	Semi-minor Axis (km)	Time-of-Flight (see)	Ellipse Orientation Angle (deg)
HII32	27.8	17.0	4.1	109
HII11	26.0	20.8	3.8	19
LII21	16.4	**3.0**	**2.0**	11
LIO31	17.2	2.7	1.7	174
LOO21	**26.6**	**4.8**	**3.7**	**0**

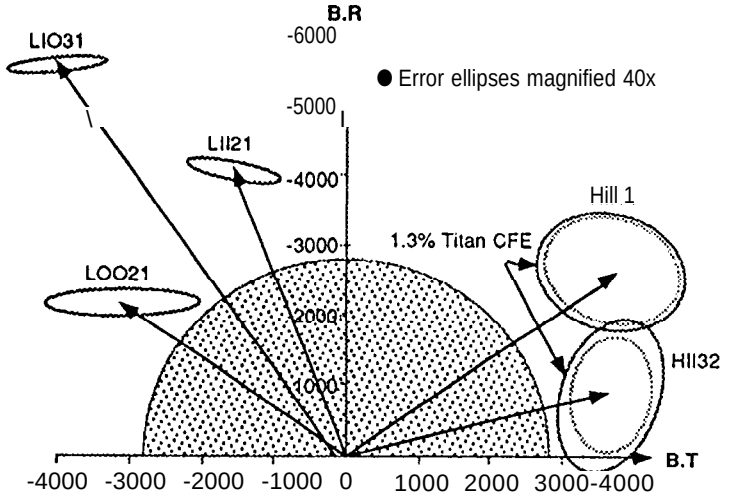

Figure 4 B-Plane Error Ellipses at T-4 days for the 5 Tour Orbits (T axis in Titan equatorial plane)

Another goal of the tour OD analysis was to determine the relative contributions of the various parameters in the filter model to the spacecraft delivery errors at Titan. An error budget of the individual contributions of the model parameters and the data types was generated for the HII32 arc.[8] The centerfinding error was changed from 1.3% to 0.75% to facilitate comparison with the low-phase data arcs*. The resulting contributions to the B-plane ellipse size and time-of-flight uncertainty at T-4 days are shown in Table 8 and Figures 5 and 6. The two largest contributors are the Titan centerfinding error consider parameters and the measurement noise for the optical data, These results underscore the need for the continuing effort to model the Titan atmosphere so that centerfinding accuracy can be improved, Satellite ephemeris uncertainty is the next largest source of error, followed by stochastic non-gravitational accelerations. The latter source of error indicates the need to model attitude control accelerations and other known non-gravitational forces acting on the spacecraft. The remaining errors are relatively small.

TABLE 8. ERROR BUDGET FOR T-4 DAY OD DELIVERY FOR **HII32** ORBIT WITH 0.750/0 TITAN CENTERFINDING ERROR

Error Type	B.T (km)	B.R (km)	Time-of-Flight (see)
Baseline	13.9	20.1	3.2
Titan centerfinding error	3.6	17.8	2,7
Satellite GM & Ephemeris	8.5	3.8	0.5
OpticalData Noise	9.7	8.3	1.3
Stochastic Non-Gravs	3.1	3.9	0.8
Radio Data Noise	1.2	1.6	0.2
Icy Satellites Centerfinding Error	1.1	1.4	0.1
Station Location	1.0	1.3	0.2
Maneuvers	1.2	1.3	0.4
Constant Non-Gravs	0.9	0.7	0.1
Media	0.3	0.3	0.1
Saturn Ephemeris	0.2	0.1	0.1
S/C State & Mass	0.1	0.1	0.01
Solar Pressure	0.0	0.0	0.001

* The only difference in the filter setup for low- and high-phase arcs was the size of the Titan centerfinding error.

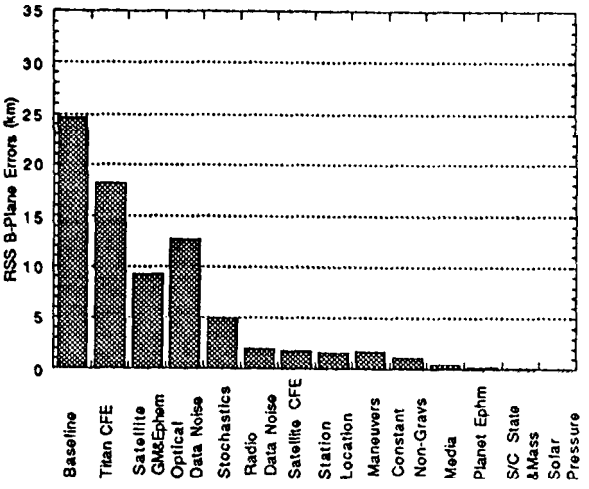

Figure 5 RSS B-Plane Error Contributions for Arc HII32 with 0.75% Titan Centerfinding Error

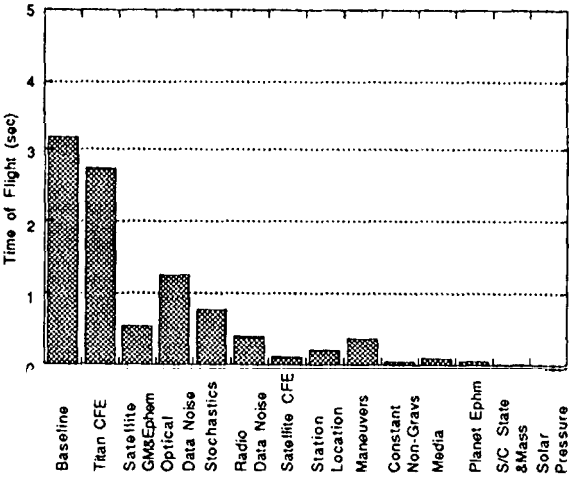

Figure 6 Time-of-Flight Error Contributions for Arc HII32 with 0.75% Titan Centerfinding Error

Titan - 2 day Knowledge for Encounter Prediction

The last opportunity for updating the onboard computer commands for Titan science observations will come at about 1 day before the encounter. The update will be based on navigation data ending at T-2 days and will provide improved estimates for instrument pointing and event timing for experiments such as occultations. Pointing predictions for planet observations will also be discussed in this section since Saturn periapsis occurs after the T-2 day cutoff. Saturn periapses falling before outbound Titan encounters occur within 24 hours after the T-2 day cutoff. In operations, Saturn pointing predictions for these cases will be based on the T-4 day OD solutions since sequence updates could not be performed in the short time between the T-2 day cutoff and Saturn periapsis. Saturn pointing predictions presented here for arcs with outbound Titan encounters may be somewhat optimistic due to the later data cutoff time. Current project requirements for predicted pointing accuracy for features on Titan or Saturn are listed in Table 6,

Titan-centered pointing errors due to navigation uncertainties were obtained by mapping the OD solutions at T-2 days forward to the encounter period. The uncertainties were transformed to the VIEW1 reference frame which has one axis along the radial direction to the target body and the other two axes along and orthogonal to the orbit angular momentum vector. The pointing errors were then computed by dividing the larger of the two uncertainty components along the axes orthogonal to the line-of-sight to Titan by the altitude to Titan at each time. In this case, altitude is defined as the distance from the spacecraft to the nadir point on the surface of Titan. The resulting prediction capability for four of the sample trajectories is shown in Table 9. Figures 7 and 8 are plots of the pointing accuracy as a function of altitude above Titan for arcs LIO31 and HII32. The plots generally show that the pointing accuracy for the part of the trajectory after the encounter is worse than that prior to the encounter due to dispersion by the encounter itself, Magnification of the pointing errors occurs when prc-encounter B-plane uncertainties are translated into uncertainty in the bending angle of the spacecraft's trajectory. Also, the shapes of the curves are considerably modulated in some instances by the shape and aspect of the spacecraft error ellipsoid as it proceeds through the encounter. The requirements for the Than pointing prediction can almost always be met for the inbound asymptote, and only partially met for the outbound asymptote.

TABLE 9. PREDICTED TITAN NADIR POINTING ACCURACY

Trajectory	POINTING ACCURACY (95% Confidence level) (mrad)			
	Range=30,000 km		Range= 20,000 km	
	Before Titan Periapsis	After Titan Periapsis	Before Titan Periapsis	After Titan Periapsis
LO021	1.2	2.8	1.7	3.8
LIO31	1.0	1.1	1.5	1.6
LII21	1.1	1.2	1.6	1.7
HII32	1.9	3.0	2.8	3.9
Requirement	1,9		2.5	

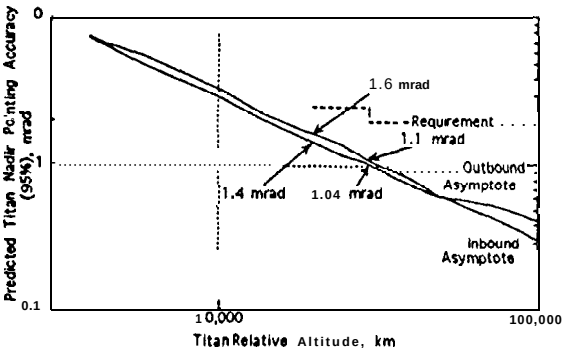

Figure 7. Predicted Titan Nadir Pointing Accuracy for Arc LIO31

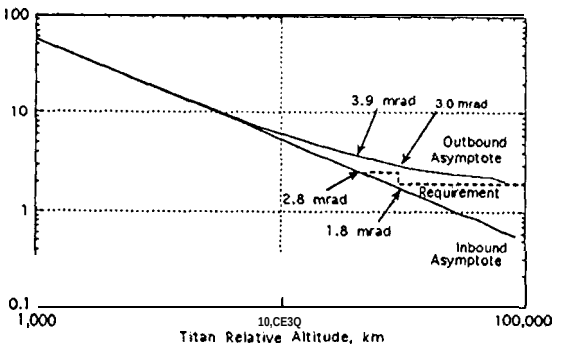

Figure 8. Predicted Titan Nadir Pointing Accuracy for Arc HII32

Saturn-relative pointing uncertainties were computed by mapping the spacecraft state uncertainties to a Saturn-centered VIEW1 coordinate system. The predicted accuracy for two of the sample trajectories is plotted as a function of time from Saturn periapsis in Figures 9 and 10. These figures reveal that the pointing accuracy around Saturn periapsis is critically dependent on the location of the Titan encounter relative to periapsis. If the Saturn penapsis occurs prior to the Titan encounter as in Figure 9, the mapping time from the data cutoff to the Saturn periapsis is very short and there arc no intervening perturbations, giving pointing accuracies less than 0.1 mrad. If, however, the Titan encounter occurs before the Saturn periapsis as in Figure 10, then the mapping times arc longer and the uncertainties are amplified by the Titan encounter. As was the case for Titan pointing requirements, the Saturn pointing requirements were not satisfied for all trajectories. The high-phase trajectory shown in Figure 10 was the worst, with pointing errors as high as 25 mrad. Some of the low-phase trajectories also had pointing errors above the 1.9 mrad requirement, although these errors were generally smaller than those for the high-phase trajectory.

The T-2 day OD delivery will also provide the final update on event times for the Titan flyby. Although there are no formal requirements on timing accuracy, Titan radar observations and other radio science experiments would be enhanced by keeping predicted timing errors as small as possible. The curves in Figure 3 show that time-of-flight uncertainties at the T-2 day cutoff are quite similar to those at the T-4 day cutoff. The values given in Table 7 for the T-4 day delivery can thus be taken to represent the baseline capability, These values are somewhat larger than the maximum error informally requested by the radio science community. Attempts to improve the time prediction accuracy arc discussed in the section on variations from the baseline case.

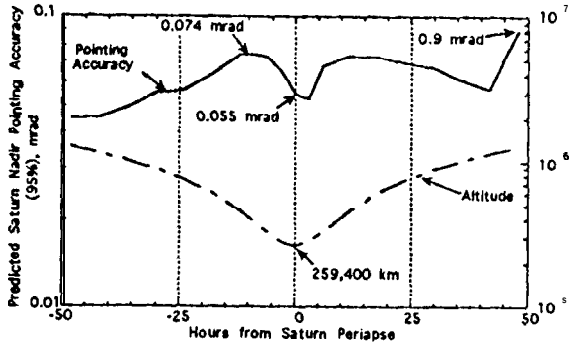

Figure 9 Predicted Saturn Nadir Pointing Accuracy for Arc LIO31

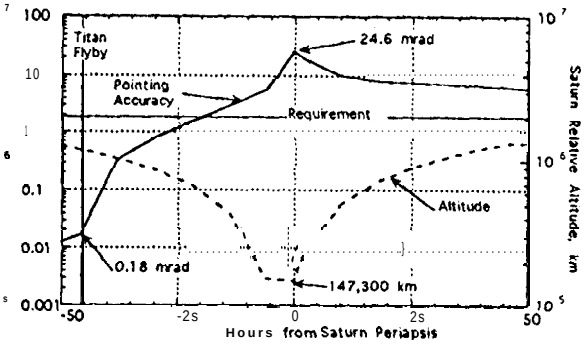

Figure 10 Predicted Saturn Nadir Pointing Accuracy for Arc HII32

Titan + 4 day Knowledge for Reconstruction

Navigation reconstruction provides the final and "best" trajectory to the science community, using data from the beginning of the arc to four days after each Titan flyby. In operations, reconstruction will be done by invoking a formal smoothing process that accounts for the presence of the stochastic parameters in the filter solution. Smoothing algorithms arc not available in the software used for this analysis. Reconstruction results were therefore generated by simply mapping the T+4 day solution backwards to previous times. Pointing errors for Titan and Saturn were computed from components of the VIEW1 mapping as described in the preceding section. Figures 11-14 illustrate the reconstructed pointing capability for Titan and Saturn for a low- and high-phase trajectory arc. Figures 11 and 12 plot Titan pointing accuracy as a function of altitude from Titan. Both of the arcs give a pointing reconstruction accuracy better than the requirement shown in Table 6, The Saturn reconstructed pointing accuracy is plotted as a function of time from Saturn periapsis in Figures 13 and 14. In this case, the accuracy requirement is met for the low-phase trajectory and for most of the time for the high-phase trajectory. There is a brief period around periapsis where the requirement is not met for the high-phase trajectory. This peak is probably an artifact of the backwards mapping assumption, This assumption is a reasonable model for reconstruction for this "first look study, but future studies will revisit reconstruction using true smoothing.

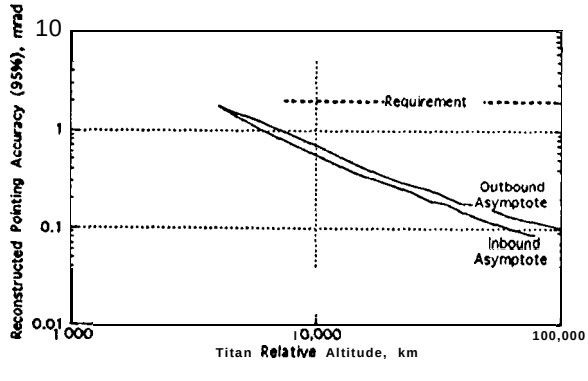

Figure 11 Reconstructed Titan Nadir Pointing Accuracy for Arc LIO31

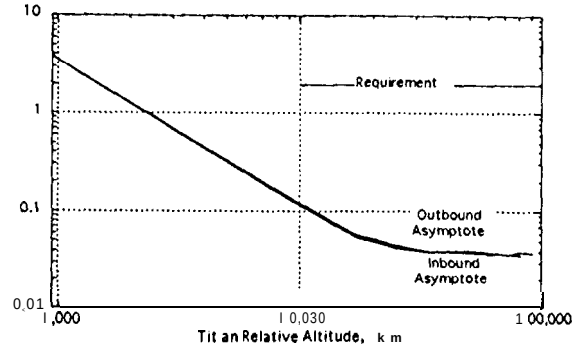

Figure 12 Reconstructed Titan Nadir Pointing Accuracy for Arc HII32

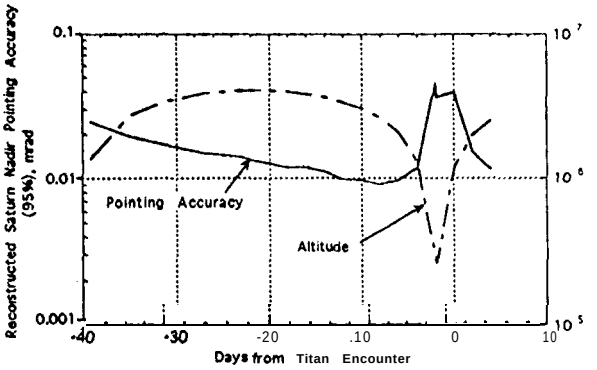

Figure 13 Reconstructed Saturn Nadir Pointing Accuracy for Arc LIO31

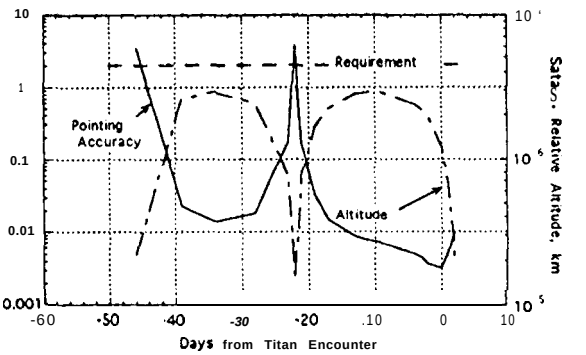

Figure 14 Reconstructed Saturn Nadir Pointing Accuracy for Arc HII32

VARIATIONS FROM BASELINE

A multitude of variations in the conditions for the baseline cases were considered in the analyses of the five sample tour trajectories. This section summarizes the more important results. Detailed results for other variations can be found in references 2 through 6. In the discussions below, emphasis is placed on changes in the OD uncertainties for the Titan Delivery Maneuver at the cutoff time 4 days prior to the encounter. The accuracy of this delivery has a major influence on the AV budget for the tour.

Optimistic Scenarios

A certain degree of conservatism was introduced into the assumptions for the baseline case since this study was done at an early stage of spacecraft and mission design. This paragraph discusses some "optimistic" variations from the baseline case where conservative restrictions are relaxed or removed. These variations are intended to provide lower bounds for OD capability during the tour; actual deliveries made in operations should always give results that are worse than those for these scenarios. The greatest benefit was obtained by removing the optical centerfinding error consider parameters from the estimation. B-plane error ellipse sizes at T-4 days were reduced to around 10 km for both low and high-phase trajectories. Corresponding time-of-flight uncertainties decreased to under 1 scc for the low-phase trajectories and below 2 see for the high-phase trajectories. Further improvements were seen by additionally removing the consider errors for the non-gravitational accelerations, station locations, and atmospheric media. The "best possible" results thus obtained were a few tenths of a second in time-of-flight uncertainty and 2-3 km in B-plane semi-major axis size at T-4 days. While these effects cannot be ignored in actual OD solutions, the results of the optimistic cases do highlight the areas for potential improvement in OD accuracy. The treatment of centerfinding errors for Titan optical data, in particular, will be addressed in an upcoming study.

Data Loss Scenarios

Another set of variations for the tour OD analysis explored the effects of removing one or more data types from the filter solutions. Some of these cases were designed to simulate a failure in the spacecraft or ground systems; others were included to investigate the need for a particular data type or to determine sensitivity to the presence of a data type at critical periods in the data arc.

Two variations that simulated spacecraft failures were the cases where only optical or radiomctric data were available. The radio-only case simulated failure of the spacecraft's camera(s) and based the OD solution on Doppler and range data alone. The optical-only case represented an extreme failure in the spacecraft's communication system which would make tracking impossible while retaining telemetry capability; optical observations of Titan and the icy satellites were used for this case. The histogram in Figure 15 shows the results of the radio-only and optical-only cases for all five sample trajectories. The bars in this chart represent the RSS of the 1σ B-plane semi-major and semi-minor axes and time-of-flight uncertainty,

assuming a V_∞ of 5,8 km/see, for the T-4 day OD delivery. Results for the baseline cases are included in the figure for comparison. Several interesting trends demonstrated in this figure are discussed in the following paragraphs.

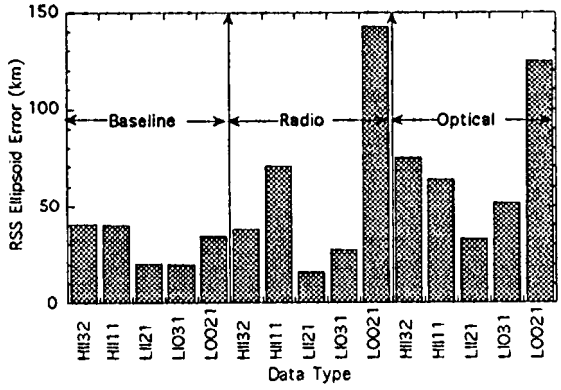

Figure 15 RSS Spacecraft State Uncertainty at T-4 days for Baseline, Radio-Only and Optical-Only Cases

As expected, errors are generally smallest for the baseline cases, which have the benefits of both data types. However, the radio data alone performs quite well for some of the trajectories. Doppler data was shown to be very effective in reducing the OD errors for arc HII32. This may have been due to a fortuitous alignment of Titan and the spacecraft near one of its Saturn periapses occurring early in the arc. This special geometry apparently enabled the filter to reduce Titan ephemeris errors for the remainder of the data arc. The radio data also performs well in cases such as LI121 where the two Titan encounters take place with Titan in roughly the same location in it's orbit about Saturn. Data from the previous Titan encounter is included in the OD solution and serves to reduce Titan ephemeris uncertainty in that part of its orbit; this local ephemeris improvement is then carried over to the second encounter allowing the Doppler data to further improve the spacecraft state uncertainties.

The performance for the optical-only cases is somewhat disappointing in that is it often worse than the baseline or radio-only cases. This poor performance can be attributed to the presence of the Titan centerfinding error consider parameters. This effect is especially noticeable for the high-phase trajectories which have a larger a priori uncertainty for these parameters. Finally, it is obvious from the figure that the optical-only and radio-only results for arc LO021 are not consistent with those for the other arcs. The reason for this difference has not yet been found, but may be uncovered in future analysis.

Overall sensitivity to ranging data was explored with cases using only Doppler and optical data for arcs LO021, LII21 and LI031. The results for these cases were virtually indistinguishable from the baseline results. The requirements for ranging data during the tour will be revised to reduce the number of measurements based on these results.

The effect of data loss in the high-activity period around a Titan flyby was investigated. These variations assumed that no data would be available for progressively longer periods centered around the time of Titan closest approach. The baseline case assumed a 20-hr gap at this time, but the new cases extended the size of the gap up to 48 hours for the LII21 trajectory. To further stress the solution, a new set of non-gravitational accelerations was added in the eight hours around closest approach to model usc of spacecraft thrusters for pointing the science instruments at Titan. The accuracy of the post-encounter OD solution at T+1 day was not significantly degraded even for the largest data gap as long as some data was available just before the T+1 day cutoff,

Previous results for both the baseline error budget and the optimistic scenarios have demonstrated that OD performance is very sensitive to the Titan centerfinding error consider parameters. Assuming that the

use of these parameters reflects the actual Titan centerfinding capability, it is reasonable to consider eliminating the Titan pictures and using optical data for the icy satellites only, This variation was run for arcs LO021, LII21 and HH11: figure 16 compares the RSS OD uncertainties at T-4 days for these cases with the corresponding baseline cases for each arc. There is improvement over the baseline cases for all arcs, but the reduction in OD uncertainty is much larger for the low-inclination arcs than for the high-inclination arc. These initial results are promising, but some issues must be addressed before this strategy is officially adopted. For instance, these cases assume that the Titan ephemeris errors can be maintained at the 10-20 km level which may not be possible without in situ optical data. ALso, the satellites' dynamic interactions were not included in the simple conic model used for this analysis. Future studies will address the ramifications of no Titan optical data in more detail.

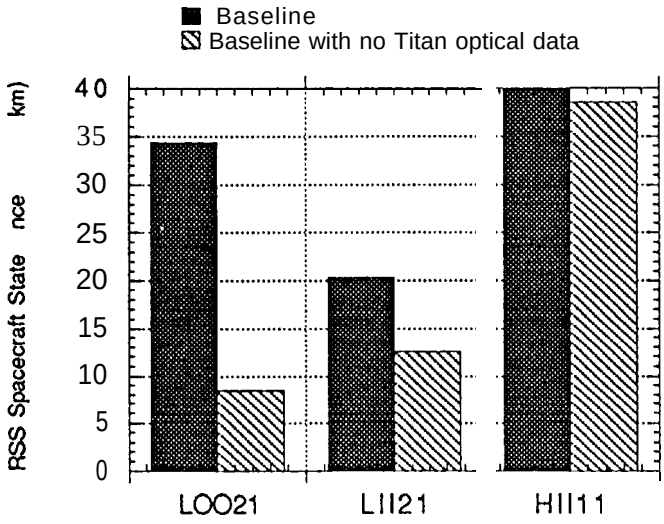

Figure 16 RSS Uncertainties at T-4 days for Baseline and Cases with No Titan Optical Data

Scenarios with Reduced Data Quantity

A few runs were made to investigate the effects of reducing the number of Titan pictures in the optical data arc for the LOO21 trajectory. These runs demonstrated that the number of Titan pictures could be decreased by a factor of 2 from that of the baseline schedule without seriously degrading OD performance for the T-4 day and T-2 day deliveries. This result is predicated on the fact that the last, highest resolution pictures before the flyby occurred at the same times for each reduced picture schedule. The resolution of the final Titan picture plays a major role in the accuracy of the OD solution; resolution, and hence, OD accuracy decreases rapidly as the final picture time is moved farther from the time of Titan closest approach. Reductions in the number of icy satellite pictures or in the amount of radiometric data were not considered for this analysis.

Scenarios using Enhanced Radiometric Data Types

The use of enhanced radiometric data types in addition to standard Doppler and range was addressed to aid in the formulation of navigation data requirements for the tour. A variety of data types were considered including precision Doppler and ranging, ADOR, differenced Doppler and ranging, counted Doppler and difference counted Doppler. Cases adding these data types were run primarily for the LII21 trajectory, with a few cases also run for the LOO21 and HII32 trajectories. These runs were designed to extract the maximum benefit from the new data types by eliminating the radiometric data consider parameters (station locations, atmospheric media effects, and quasar locations), scheduling frequent measurements, and using optimistic values for the data weights. Even under these favorable conditions, the Titan-relative spacecraft

state uncertainties did not improve significantly in the last ten days prior to the flyby. B-plane ellipse sizes at the T-4 day cutoff for runs using these data types were very close to those for the baseline case. In contrast, uncertainties relative to the Saturn barycenter did improve dramatically in two cases. Excellent performance was obtained using differenced counted Doppler. Unfortunately, the improvement disappeared when the consider parameters were put back in the estimation at the baseline levels. ADOR weighted at 1 cm also performed well even in the presence of the consider parameters. However, the 1 cm measurement accuracy is beyond the capability of the current system. Substantial effort would have to be expended to correctly implement and calibrate either of these data types in actual operations. There arc no current navigation requirements for Saturn-relative trajectory accuracy that could justify the cost of such an effort. Previous requirements for enhanced radiometric data types during the Saturn tour have been dropped based on the results of these variations.

Although not a formal requirement, timing knowledge on the order of 1 second or less is desired by the radio science community to obtain high quality data during Titan occultations of the spacecraft. Preliminary runs for the LH21 arc indicated that time-of-flight uncertainties between 1 and 2 seconds could be obtained by using high-precision Doppler or range. Additional variations were run for both the LII21 and LI031 trajectories to explore the effects of using Ka band Doppler on the timing uncertainties. The higher accuracy available with Ka band Doppler was simulated by setting the data weight at 0.01 mm/see for a 60 sec measurement. Timing uncertainties under 1 second were achieved for the cases where all consider parameters were removed from the estimation. Cases that included only optical centerfinding error consider parameters or radiometric data consider parameters yielded intermediate values of 1 to 2 seconds. Other runs revealed that the time-of-flight uncertainty increases when stochastic non-gravitational accelerations are omitted and that it can vary considerably even within a single pass of data. These experiments show that careful spacecraft modeling and proper data calibration are necessary to reduce timing uncertainties to the l-second level using high accuracy Doppler. A reversal of the above-mentioned decision to eliminate enhanced data types cannot be justified based on these results. Adding high-precision Doppler to the set of required navigation data types will be reconsidered if a timing accuracy limit is officially adopted by the project.

NUMERICAL PRECISION CONSIDERATIONS

Unexpected difficulties arose with some of the trajectories when attempting to map covariance matrices through two Titan encounters. Numerical problems with the pseudo-epoch state filter formulation were manifested by negative diagonal elements appearing in the covariance matrix when mapping through the second Titan flyby and/or a Saturn periapsis. A singular-value decomposition (SVD) analysis indicated that the transition and covariance matrices became ill-conditioned when stochastic non-gravitational accelerations were included in the estimations The instability in the transition matrix is illustrated in Figure 17 which plots the singular values and condition number* of the mapped diagonal covariance for a trajectory with two Titan encounters as a function of time from the epoch for the filter run. The condition number increases from 10^7 to 10^{14} at the time of the first encounter, after which it approaches the machine's limit for numerical precision. Figures 18 and 19 plot the same parameters for the unmapped, fully correlated covariance matrix for cases with and without stochastic non-gravitational accelerations (non-gravs). The condition number for the case with stochastic non-gravs was about 1023; in the absence of stochastic non-gravs it decreased to about 10^{14}.

One strategy employed to work around this problem was to eliminate the errors from stochastic non-gravs while increasing the errors from the constant non-gravs. Another strategy retained the stochastic non-gravs but shortened the data arc so that it contained only a single encounter. Neither of these strategies was satisfactory — the first was not a realistic model of Spacecraft dynamics and the second violated the desired operations strategy of having two Titan encounters in the data arc. Satisfactory results were later obtained using the original filter setup for one of the sample arcs when the analysis software was modified to map a factorized covariance rather than the full matrix, This modification was analogous to mapping the square root of the covariance and effectively decreased the exponents of the condition number by half. The operational OD software already uses a square-root formulation for mapping and is expected to behave like

* The condition number is the ratio of the largest to the smallest singular value for a matrix.

the modified analysis software. However, there is still some concern that the condition number may become unacceptably large for other data arcs, particularly those with multiple spacecraft revolutions around Saturn between Titan encounters, This possibility will be investigated in future analysis.

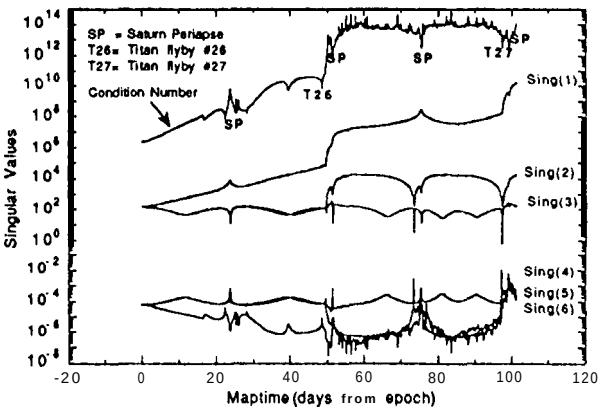

Figure 17 SVD for Mapped Diagonal Covariance Matrix for a Trajectory Arc with 2 Titan Flybys

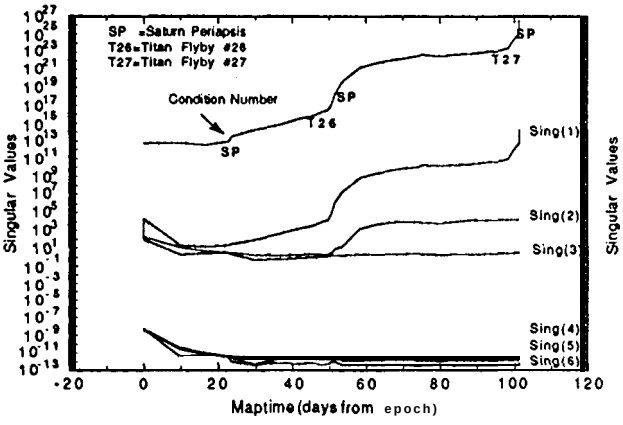

Figure 18 SVD for Covariance Matrix *with* Stochastic Non-Gravs for Trajectory Arc with 2 Titan Flybys

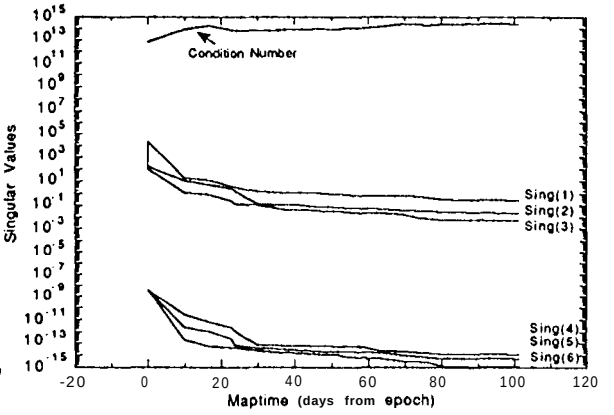

Figure 19 SVD for Covariance Matrix *without* Stochastic Non-Gravs for Trajectory Arc with 2 Titan Flybys

CONCLUSIONS

The initial round of OD analyses for the Cassini Saturn tour has investigated trajectories with both low and high inclinations and low and high solar phase angles for the satellite images. Simulations have demonstrated the capability to deliver the spacecraft to a Titan encounter with uncertainties between 20 and 30 km using only standard 2-way Doppler, ranging and optical observations of Titan and the other icy satellites. This capability satisfies the proposed requirements based on fuel budget considerations, but there is little margin for some cases such as the high-inclination orbits. Current project requirements for predicted and reconstructed pointing accuracy at Titan and Saturn were not met for some cases. Requirements for reconstructed pointing accuracies were satisfied more often than those for predicted accuracies, especially for Titan. The primary source of trajectory knowledge error was shown to be the centerfinding errors associated with the Titan optical data.

Experiments were performed using combinations of data types other than the baseline set of Doppler, range and optical. The elimination of ranging data had almost no effect on the baseline results. Standard Doppler and range data alone performed satisfactorily for most trajectories. Little justification was found for extending the data set to include enhanced radiometric data types such as ADOR. The simulations showed that improved OD performance would only be obtained at the expense of implementing better spacecraft models and data calibration procedures. OD performance for cases using only optical data was sometimes worse than for the baseline case due to the presence of the Titan centerfinding error consider parameters. Reduction in spacecraft delivery uncertainties when Titan images were eliminated from the optical data arc can be attributed to the absence of these consider parameters.

Much work remains to be done to better understand OD performance during the Cassini Saturn tour. The diversity of results from the different trajectory arcs has not been adequately explained. A better characterization of the differences induced by orbital geometry will be obtained by extending the set of sample tour trajectories. Furthermore, it is unclear whether the "average" capability is sufficient to meet the tour OD requirements. A primary objective of new analysis is to demonstrate a somewhat larger margin between OD requirements and capabilities, An important step toward this goal is to improve the centerfinding accuracy for optical images of Titan. Another important objective is to demonstrate that two Titan encounters can always be reliably handled in a single data arc, Future work should also incorporate improved satellite modeling, using an integrated satellite ephemeris with its associated variational partial derivatives.

ACKNOWLEDGMENTS

The authors thank Jeremy B. Jones of JPL for his work on pointing prediction and reconstruction capabilities and for his many comments and suggestions during the course of this analysis. Thanks also to Francis M. Stienon of JPL for maintaining the ATHENA software set used for this analysis.

The research described in this paper was performed at the Jet Propulsion Laboratory, California Institute of Technology, under contract with the National Aeronautics and Space Administration.

REFERENCES

1. Taylor, A.H., Ionasescu, R., and Vaughan, R. M., "A First Look at Orbit Determination for the Cassini Mission, Part 1: Inner Solar System through Probe Delivery", Paper AAS 93-608, AAS/AIAA Astrodynamics Specialist Conference, Victoria, B.C., Canada, 16-19 August 1993.
2. Vaughan, R. M., "OD Analysis Results for a Typical Low-phase Orbit in Cassini Saturn Tour," JPL Interoffice memorandum 314.8-852 (internal document), Jet Propulsion Laboratory, Pasadena, California, 6 November 1992.
3. Taylor, A. H., "Orbit Determination for the Low-phase Portion of the Cassini Tour: Two Representative Data Arcs," JPL Interoffice memorandum 314.3-1029 (internal document), Jet Propulsion Laboratory, Pasadena, California, 17 December 1992.
4. Taylor, A. H., "Titan Revisited: Some Quick OD Results for Cassini,", JPL Interoffice memorandum 314.3-1043 (internal document), Jet Propulsion Laboratory, Pasadena, California, 6 April 1993.
5. Ionasescu, R., "Orbit Determination Results for a High Sun Phase, Higher Inclination Orbit in the Cassini Saturn Tour," JPL Interoffice memorandum 314.3-1053 (internal document), Jet Propulsion Laboratory, Pasadena, California, 12 May 1993.
6. Ionasescu, R., "Orbit Determination Results for a *High* Sun Phase, *High* Inclination Orbit in the Cassini Saturn Tour," JPL Interoffice memorandum 314.3-1064 (internal document), Jet Propulsion Laboratory, Pasadena, California, 27 August 1993.
7. Jones, J. B., "Cassini Navigation Pointing Capability Estimate", JPL Interoffice Memorandum 314.1-0690/JBJ (internal document), Jet Propulsion Laboratory, Pasadena, California, 15 June 1993.
8. Ionasescu, R., "Error Contributions to the Spacecraft Delivery Errors Using the ATHENA Evaluation Mode," JPL Interoffice Memorandum 314.3-1063 (internal document), Jet Propulsion Laboratory, Pasadena, California, 1 July 1993.

APPENDIX

Planet or satellite approach trajectories arc typically described in aiming plane coordinates referred tom "B-plane" coordinates (see Figure A-l). The B-plane is a plane passing through the body center and perpendicular to the asymptote of the incoming trajectory (assuming 2-body conic motion). The "B-vector" is a vector in that plane, from the body center to the piercing-point of the trajectory asymptote, The B-vector specifies where the point of closest approach would be if the target body had no mass and did not deflect the flight path. Coordinates are defined by three orthogonal unit vectors, ***S***, *T*, and ***R*** with the system origin at the center of the target body. The ***S*** vector is parallel to the spacecraft V_∞ vector (approximately the velocity vector relative to the target body at the time of entry into its gravitational sphere of influence). ***T*** is arbitrary, but typically specified to lie in the ecliptic plane (the mean plane of the Earth's orbit), or in a body equatorial plane. Finally, *R* completes an orthogonal triad with ***S*** and *T*.

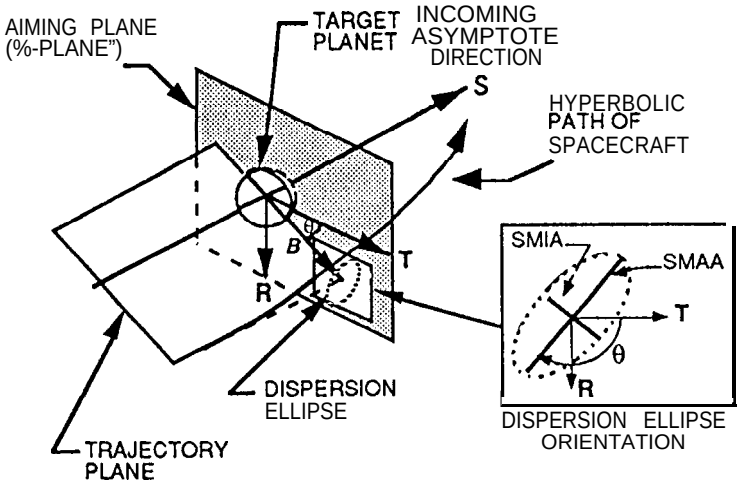

Figure A-1 Aiming Plane Coordinate System Definition

Trajectory errors in the B-plane are often characterized by a one-sigma dispersion ellipse as shown in Figure A-1. SMAA and SMIA denote the semi-major and semi-minor axes of the ellipse; θ is the angle measured clockwise from the T axis to SMAA. Dispersions normal to the B-plane are typically given as a one-sigma *time-of-flight* error, where time-of-flight specifies what the time to encounter would be from some given epoch if the magnitude of the B-vector were zero. Alternatively, these dispersions arc sometimes given as a one-sigma distance error along the S direction, numerically equal to the time-of-flight error multiplied by the magnitude of the V_∞ vector,